

Computational Design of Axion Insulators Based on 5d Spinel Compounds

Xiangang Wan,¹ Ashvin Vishwanath,^{2,3} and Sergey Y. Savrasov⁴

¹National Laboratory of Solid State Microstructures and Department of Physics, Nanjing University, Nanjing 210093, China

²Department of Physics, University of California, Berkeley, California 94720, USA

³Materials Sciences Division, Lawrence Berkeley National Laboratory, Berkeley, California 94720, USA

⁴Department of Physics, University of California, Davis, One Shields Avenue, Davis, California 95616, USA

(Received 23 March 2011; published 5 April 2012)

Based on density functional calculation using the local density approximation + U method, we predict that osmium compounds such as CaOs_2O_4 and SrOs_2O_4 can be stabilized in the geometrically frustrated spinel crystal structure. They show ferromagnetic order in a reasonable range of the on-site Coulomb correlation U and exotic electronic properties, in particular, a large magnetoelectric coupling characteristic of axion electrodynamics. Depending on U, other electronic phases including a 3D Weyl semimetal and Mott insulator are also shown to occur.

DOI: 10.1103/PhysRevLett.108.146601

PACS numbers: 72.25.Hg, 71.15.Mb, 73.20.-r, 85.75.-d

Recently, theoretical work has played a key role in the discovery of novel topological insulators (TIs), where time reversal symmetry protects unusual surface states which could lead to electronic devices with new functionalities [1–3]. Unlike other fields of condensed matter physics, where most compounds are found haphazardly, here a number of new materials have been suggested based on band structure calculations [4–6], some of which have been confirmed experimentally [7,8].

In addition to these unusual electronic properties, introducing magnetic order on the surface of TIs can gap the surface states leading to completely insulating behavior. Here, novel phenomena such as the half quantum Hall effect [9] and the quantized magnetoelectric effect [10] appear. The latter is parameterized by the quantized value of the axion electrodynamics parameter $\theta = \pi$ [10,11]. When time reversal symmetry as well as spatial symmetries like inversion are broken in the bulk, the θ parameter is no longer quantized [12,13]. However, in most known materials, it is extremely small, e.g., $\theta = 10^{-3}$ and 10^{-4} in Cr_2O_3 and BiFeO_3 , respectively [13]. Thus, achieving large values of the θ parameter, even in the absence of quantization, is an important materials challenge. For sufficiently large $\theta > \pi/2$, it has been proposed that magnetic domain walls will be associated with conducting channels at the sample surface [14]. Recent experimental progress in introducing magnetism via dopants [15,16] in Bi_2Se_3 has been reported, as well as tuning of a chemical potential into a small gap at the surface states [16]. Ideally, however, magnetic topological insulators would combine band topology with intrinsic magnetic order, leading to large surface energy gaps. Unfortunately, most of the known or proposed TIs involve *p*-electron orbitals, whose Coulomb interaction is weak and cannot support magnetism. Elements with 3*d* and 4*d* electrons do have large electronic correlations but only small spin-orbit coupling. While both strong Coulomb interaction and large spin-orbit coupling

are found in 4*f* and 5*f* electron systems, they usually form narrow energy bands, thus making it also hard to realize the TI state of matter (see [17] for an exception).

Because of the interplay of strong spin-orbit coupling and moderate electronic correlations, very recently systems with 5*d* electrons have received a lot of research attention [18–23]. It has been suggested that pyrochlore iridates exhibit novel phases such as, e.g., TI [21,22] and topological semimetal [23] behavior. As in pyrochlores $\text{A}_2\text{B}_2\text{O}_7$, spinel compounds AB_2O_4 have their four *B* sites forming a corner-sharing tetrahedral network. Furthermore, it may be expected that 5*d* systems in the spinel structure will be more tunable by pressure, external fields, or doping as compared to the closely packed pyrochlore lattice. Previous studies suggested that the electronic d^5 configuration can realize an insulating state in 5*d* compounds [19]. Based on valence arguments, we therefore focus on spinel osmates AOs_2O_4 (*A* is an alkali metal element such as Mg, Ca, Sr, or Ba) and investigate their electronic structure and magnetic properties by using theoretical density functional calculations. Our numerical results reveal that the spinel structure can at least be a metastable crystallographic state for 5*d* elements which is additionally supported by a very recent synthesis of an empty iridium spinel compound Ir_2O_4 [24]. Most interestingly, we find that the ferromagnetic configuration is the ground state of the candidate orders considered and the electronic properties are sensitive to the *A* site. Depending on the strength of the Coulomb correlation, they show some exotic properties, and for the range of U's relevant to the Os element, we predict CaOs_2O_4 and SrOs_2O_4 to behave as magnetic axion insulators with $\theta = \pi$. The quantized value is protected by the inversion symmetry of the lattice. However, since the surfaces break inversion, typically they are gapped, allowing us to define θ . Unlike other proposals for generating large θ , which exploit proximity to a topological insulator state [16], here a

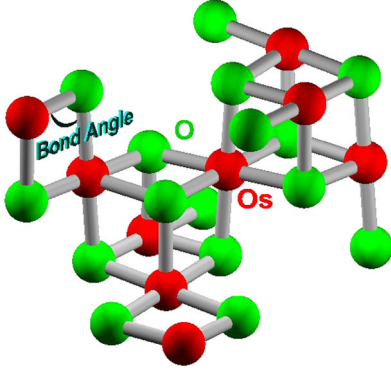


FIG. 1 (color online). Fragment of spinel crystal structure AOs_2O_4 (only Os and O atoms are shown) with the Os-O-Os angle being optimized.

generalized parity criterion [25,26] allows us to obtain large θ even when no proximate TI state exists.

We perform our electronic structure calculations for the spinel osmates based on the local spin density approximation (LSDA) to density functional theory with the full-potential, all-electron, linear-muffin-tin-orbital method [27]. Despite the fact that the $5d$ orbitals are spatially extended, recent theoretical and experimental work has given evidence on the importance of Coulomb interactions in $5d$ compounds [19]. We utilize the LSDA + U scheme [28], which is adequate for searching magnetically ordered insulating ground states [29] by taking into account the effect of Coulomb repulsion, and vary parameter U between 0 and 1.5 eV. Very recently, using the same scheme, we successfully predicted pyrochlore iridates to have an all-in or all-out noncollinear magnetic ordering [23], and our predictions have been confirmed by subsequent theoretical [30] and experimental [31] publications. We use a $24 \times 24 \times 24$ k mesh to perform Brillouin zone integration and switch off symmetry operations in order to minimize possible numerical errors in studies of various (non)collinear configurations. As the experimental lattice parameters are not available, we search for the stable crystal structures by locating the minimum in the calculated total energy as a function of the lattice constant and internal atomic coordinates.

The spinel structure (see Fig. 1) forms space group $Fd\bar{3}m$. In order to allow its relaxation, we change the lattice constant from 13 to 18 a.u. and vary the Os-O-Os bond angle from 90° to 120° with a step of 1° . We confirm that the choice of Coulomb U has only a small effect on the lattice and list the lowest energy structures obtained by LSDA + SO ($U = 0$) calculations in Table I. The structural stability has further been checked by studying various energy surfaces, chemical stability with possible reactants, and other crystal structures and by calculating the phonon spectrum. This is discussed in Ref. [32]. For comparison, in Table I we also list the same parameters for the pyrochlore iridate $\text{Y}_2\text{Ir}_2\text{O}_7$. We see that the A -site element has a

TABLE I. Theoretically determined lattice parameters of spinel osmates. Angle denotes the Os-O-Os bond angle; Os-O and Os-Os denote the nearest neighbor Os-O bond length and Os-Os bond length, respectively.

| | Angle | Os-Os | Os-O |
|-----------------------------------|---------------|--------------------|--------------------|
| CaOs_2O_4 | 98.5° | 3.07 \AA | 2.04 \AA |
| SrOs_2O_4 | 94.6° | 3.12 \AA | 2.05 \AA |
| BaOs_2O_4 | 103.1° | 3.28 \AA | 2.11 \AA |
| $\text{Y}_2\text{Ir}_2\text{O}_7$ | 129.7° | 3.60 \AA | 1.99 \AA |

considerable effect on the Os-O bond angle and its length. As we discuss below, this allows us to control the electronic structure in osmates and design exotic topological phases.

Our calculation predicts MgOs_2O_4 to be always metallic. We therefore do not discuss this compound here and concentrate our study on CaOs_2O_4 . Its band structure from nonmagnetic LSDA + SO calculation is found to be metallic and shown in Fig. 2(a). The energy bands around the Fermi level appear as $J_{\text{eff}} = 1/2$ states similar to the ones found in Sr_2IrO_4 [19] and also in $\text{Y}_2\text{Ir}_2\text{O}_7$ [23], where a metal rather than the interesting topological insulator scenario of Ref. [21] was obtained due to a 2-4-2 sequence of degeneracies at the Γ point. As the importance of electronic correlations for $5d$ orbitals has been recently emphasized [19] and estimates for the values of U have been recently obtained between 1.4 and 2.4 eV in layered $\text{Sr}_2\text{IrO}_4/\text{Ba}_2\text{IrO}_4$ [33], we perform LSDA + U + SO calculations. Although the accurate value of U is not known for spinels, we generally expect screening to be larger in 3D systems than that of 2D systems like Sr_2IrO_4 . Furthermore, the Os-Os bond length is shorter than that of $\text{Y}_2\text{Ir}_2\text{O}_7$, and one can expect that the U in CaOs_2O_4 is

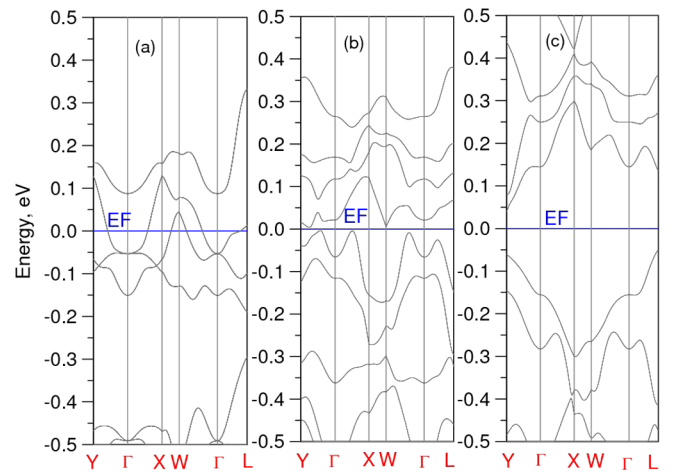


FIG. 2 (color online). Electronic band structure of CaOs_2O_4 shown along high symmetry direction. (a) LSDA + SO; (b) LSDA + SO + U , with $U = 0.5$ eV; (c) LSDA + SO + U , with $U = 1.5$ eV.

also smaller than in $\text{Y}_2\text{Ir}_2\text{O}_7$. We therefore believe that the U is in the range between 0.5 and 1.5 eV. As in the pyrochlore structure, the Os spinel sublattice is geometrically frustrated. Naively, one may expect that the magnetic configuration of CaOs_2O_4 is also noncollinear as recently found in $\text{Y}_2\text{Ir}_2\text{O}_7$ [23]. To search for possible magnetic ground states, we perform calculations by starting with a number of different collinear and noncollinear magnetic configurations including ferro- (FM) and antiferromagnetic collinear (010), (110), and (111), as well as noncollinear all-in or all-out, 2-in and 2-out, 3-in and 1-out, and some perpendicular configurations promoted by Dzyaloshinsky-Moriya interactions [34]. We find that when U is less than 1.3 eV, only the FM-(010) configuration retains its initial input magnetization direction; in all other configurations, the moments depart from their input orientation. We also consider a 2-up, 2-down state, which is suggested by the strong coupling limit where Os-O bonds are nearly 90° . As shown in Ref. [35], this leads to a “Kitaev-type” ferromagnetic interaction for spin components perpendicular to the plane. Although this structure is found to be stable for $U < 0.8$ eV, it is higher in energy than the ferromagnetic state as shown in Table II. Regardless of the value of U , the FM configuration with magnetization along (010) is found to be the ground state, and the energy difference between this and other configurations is quite large. To find magnetically ordered solutions, here we restricted our search by the original unit cell. Although identifying more complex (such as incommensurate) forms of order recently discussed in pyrochlore osmates $\text{Cd}_2\text{Os}_2\text{O}_7$ [36] or in layered SrCr_2O_4 and CaCr_2O_4 [37] would require a full analysis of the momentum-dependent magnon spectrum, we have checked for possible nesting of paramagnetic Fermi surfaces in our proposed Os spinels but cannot detect any strong features. This can be an indication that the incommensurate order is unlikely.

By examining lattice parameters in Table I, we see that the main difference between pyrochlore iridates and spinel osmates is the Os-O-Os bond angle and the Os-Os bond length. Because of the extended nature of $5d$ orbitals, the

$5d-2p$ hybridization is strong and important for the interatomic exchange interaction. In $\text{Y}_2\text{Ir}_2\text{O}_7$, the Ir-O-Ir bond angle is much larger than 90° , and Ir-O-Ir antiferromagnetic superexchange interaction is dominant. This results in a strong magnetic frustration and noncollinear ground state magnetic configuration [23]. In contrast to pyrochlores, the Os-O-Os angle in spinel osmates is close to 90° , while Os $5d$ orbitals have stronger overlap, making a direct ferromagnetic exchange important for CaOs_2O_4 .

For the values of $U = 0.5$ and 1.5 eV, electronic band structures along high symmetry lines appear to be insulating as shown in Figs. 2(b) and 2(c), respectively. To check a possibility of the gap closure and the metallic behavior away from the high symmetry lines of the Brillouin zone, we perform the calculation with a $100 \times 100 \times 100$ k mesh. This very dense k mesh confirms that both $U = 0.5$ and 1.5 eV calculations show the band gaps of 0.01 and 0.08 eV, respectively.

In order to examine whether the system becomes an axion insulator, we recall that similar to the Fu and Kane criterion [5], which is designed for nonmagnetic systems with inversion symmetry, one can still use the parity eigenvalues for the states at eight time reversal invariant momenta (TRIM) in order to classify the magnetic insulators with inversion symmetry and evaluate the magnetoelectric coupling [25,26]: $\theta = \pi M (\text{mod } 2)$, where $M = (\sum_k N_i)/2$, and N_i is the number of occupied states at the TRIM points i with odd parity. This allows us to analyze their topological electronic properties based on the parities of occupied bands. One must also verify that the Chern number of the bands vanishes, to define the magnetoelectric coupling, which can be done by studying the evolution of the band structure from a trivial insulating state. The local environment of the Os ion in spinels is oxygen octahedron, and the crystal-field splitting of Os $5d$ states is large, which makes the e_g band higher (about 2 eV) than the Fermi level. The bands close to the Fermi level are mainly contributed by t_{2g} mixed with O $2p$ orbitals. There are 4 Os per unit cell; thus, the number of t_{2g} bands is 24. If all of the 24 t_{2g} bands are fully occupied, the system cannot possess any topologically nontrivial properties. Noticing that Os occurs in its 3^+ valence, for an insulator to occur, there are 20 occupied and 4 empty t_{2g} bands. Thus, instead of analyzing 20 occupied bands, we alternatively look at the parities of 4 empty bands.

For the spinel lattice, the eight TRIM points are Γ , X , Y , Z , and four L points. For the Γ point, all of the t_{2g} bands possess even parity, while for X , Y , and Z points, 2 of the 4 empty bands have even parity and the other 2 bands possess odd parity. Thus, regardless of the value of U , the summation of the number of empty t_{2g} states with odd parities at Γ , X , Y , and Z points is 6. On the other hand, the Coulomb interaction has a significant effect on the parities of the bands around the L points. This is shown in Table III, where the summation of the number of the odd states are

TABLE II. The spin $\langle S \rangle$ and orbital $\langle O \rangle$ moment (in μ_B) as well as the total energy E_{tot} per unit cell (in meV) for several selected magnetic configurations of CaOs_2O_4 as calculated by using the LSDA + U + SO method with $U = 0.5$ eV. (E_{tot} is defined relative to the ground state.) DMI is a coplanar configuration predicted for one sign of Dzyaloshinsky-Moriya interaction in Ref. [34].

| Configuration | (010) | All-in or all-out | 2-in and 2-out | 2-up and 2-down | DMI |
|------------------------|-------|----------------------|-------------------|--------------------|------|
| $\langle S \rangle$ | 0.59 | 0.30 | 0.40 | 0.25 | 0.35 |
| $\langle O \rangle$ | 0.14 | 0.21 | 0.22 | 0.14 | 0.16 |
| E_{tot} (meV) | 0.00 | 290 | 280 | 518 | 351 |

TABLE III. Calculated parities of states at TRIM for CaOs_2O_4 . Only 4 empty t_{2g} bands are shown in order of increasing energy. L_x denotes $2\pi/a(-0.5, 0.5, 0.5)$, L_y denotes $2\pi/a(0.5, -0.5, 0.5)$, L_z denotes $2\pi/a(-0.5, 0.5, 0.5)$, and L denotes $2\pi/a(0.5, 0.5, 0.5)$.

| | L_x | L_y | L_z | L |
|----------------------|-------|-------|-------|------|
| $U = 0.5 \text{ eV}$ | ++++ | ++++ | ++++ | ---- |
| $U = 1.5 \text{ eV}$ | -+++ | -+++ | -+++ | +--- |

6 and 4 for $U = 1.5$ and 0.5 eV , respectively. Therefore, for $U = 1.5 \text{ eV}$, we have $\theta = 0$, which corresponds to a normal insulator. However, for $U = 0.5 \text{ eV}$, we have $\theta = \pi$, which leads us to the axion insulator with novel magnetoelectric properties.

Topological insulators must be separated from trivial insulators by a semimetallic state [23], with 3D Dirac- or Weyl-like dispersion. To find the boundary between semimetal and axion insulator as well as between semimetal and Mott insulator, we perform calculations for a number of intermediate values of U . While the validity of the LDA + U scheme for semimetallic states can be questioned in general, recent studies of graphene [38] show a very good agreement between electronic structure theory and angle-resolved photoemission experiments. This hints that the mean field approach can be a good starting point for describing band crossings such as Dirac points or Weyl points considered in our work. Our calculations for U 's varying from 1.0 to 1.3 eV show that there are 3D Weyl crossings close to $(0.02, x, 0.02)2\pi/a$ and its symmetry related points of the Brillouin zone, where the value of x changes with U . With both decreasing and increasing U , the Weyl points move and annihilate by meeting with each other, thus opening the energy gap and forming either the $\theta = \pi$ axion insulator or normal insulator, respectively.

In summary, our electronic phase diagram (see Fig. 3) for $U < 0.4 \text{ eV}$ predicts CaOs_2O_4 to be a metal; for $0.4 < U < 0.9 \text{ eV}$, an axion insulator; for $0.9 < U < 1.4 \text{ eV}$, a topological semimetal metal; for $U > 1.4 \text{ eV}$, a Mott insulator. Note that, as in the cubic pyrochlore iridates [23], symmetry dictates that the eight Weyl points realized in this system are all exactly at the Fermi energy. To see the sensitivity of these results to the lattice parameters, we

perform calculations with increasing and decreasing the volume by 6%, as well as adjusting the internal coordinates and performing small changes in the Os-O-Os bond angle. We confirm that, while there are some little changes in calculated energy bands, our predictions on axion-insulator behavior are robust.

By replacing Ca by Sr, both the Os-O-Os bond angle and the bond length will change as shown in Table I. However, the same as CaOs_2O_4 , SrOs_2O_4 shows the same rich phase diagram as a function of U .

We finally study BaOs_2O_4 , which has both the largest bond angle and bond length as shown in Table I. These differences significantly affect its band structure: The LDA + SO calculation with $U = 0$ gives that at the Γ point the eight $J_{\text{eff}} = 1/2$ states have degeneracies 4-2-2 and not 2-4-2 as found in Ca and Sr cases. Note that this sequence of levels is the same as recently suggested by Pesin and Balents to realize a topological insulating scenario in pyrochlore iridates [21]. Unfortunately, the bands crossing the Fermi level exist and cannot be removed by slightly adjusting the lattice constant. The same with CaOs_2O_4 and SrOs_2O_4 , considering the Coulomb interaction U will induce magnetism, but we do not find an axion-insulator or Weyl-metal state for BaOs_2O_4 for any reasonable U .

In summary, using density functional based electronic structure calculations, we have found that, depending on the strength of the Coulomb correlation among the $5d$ orbitals, several exotic electronic phases may be realized in Os-based spinel compounds. In particular, a magnetic topological insulating phase (axion insulator) may be realized in CaOs_2O_4 and SrOs_2O_4 with a large orbital magnetoelectric parameter $\theta = \pi$. This research suggests that new functionalities, such as controlling electrical [14] and optical [39] properties via magnetic textures, can be found in the new $5d$ spinel materials that we proposed.

X.W. acknowledges support by National Key Project for Basic Research of China (Grants No. 2011CB922101 and No. 2010CB923404), NSFC under Grants No. 91122035, No. 10974082, and No. 11174124, and PAPD. S.Y.S. acknowledges support by DOE SciDAC Grant No. SE-FC02-06ER25793 and thanks Nanjing University for the kind hospitality during his visit to China. The work at Berkeley was supported by the Office of BES, Materials Sciences Division of the U.S. DOE under Contract No. DE-AC02-05CH1123.

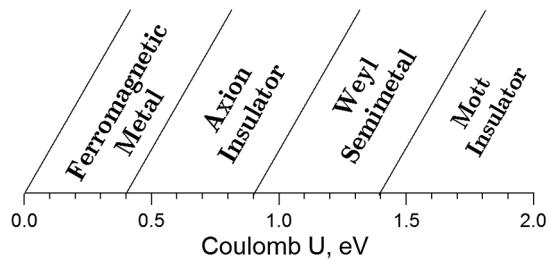


FIG. 3. Sketch of the predicted phase diagram for spinel osmates.

- [1] X.L. Qi and S.C. Zhang, *Phys. Today* **63**, No. 1, 33 (2010).
- [2] M.Z. Hasan and C.L. Kane, *Rev. Mod. Phys.* **82**, 3045 (2010).
- [3] J.E. Moore, *Nature (London)* **464**, 194 (2010).
- [4] B.A. Bernevig, T.L. Hughes, and S.C. Zhang, *Science* **314**, 1757 (2006).
- [5] L. Fu and C.L. Kane, *Phys. Rev. B* **76**, 045302 (2007).

- [6] H. Zhang, C.-X. Liu, X.-L. Qi, X. Dai, Z. Fang, and S.-C. Zhang, *Nature Phys.* **5**, 438 (2009).
- [7] D. Hsieh, D. Qian, L. Wray, Y. Xia, Y. S. Hor, R. J. Cava, and M. Z. Hasan, *Nature (London)* **452**, 970 (2008).
- [8] Y. Xia *et al.*, *Nature Phys.* **5**, 398 (2009).
- [9] L. Fu, C. L. Kane, and E. J. Mele, *Phys. Rev. Lett.* **98**, 106803 (2007).
- [10] X. L. Qi, T. Hughes, and S. C. Zhang, *Phys. Rev. B* **78**, 195424 (2008).
- [11] F. Wilczek, *Phys. Rev. Lett.* **58**, 1799 (1987).
- [12] A. M. Essin, J. E. Moore, and D. Vanderbilt, *Phys. Rev. Lett.* **102**, 146805 (2009).
- [13] A. Malashevich, I. Souza, S. Coh, and D. Vanderbilt, *New J. Phys.* **12**, 053032 (2010).
- [14] J. C. Y. Teo and C. L. Kane, *Phys. Rev. B* **82**, 115120 (2010).
- [15] L. A. Wray, S.-Y. Xu, Y. Xia, D. Hsieh, A. V. Fedorov, Y. S. Hor, R. J. Cava, A. Bansil, H. Lin, and M. Z. Hasan, *Nature Phys.* **7**, 32 (2011).
- [16] Y. L. Chen *et al.*, *Science* **329**, 659 (2010).
- [17] M. Dzero, K. Sun, V. Galitski, and P. Coleman, *Phys. Rev. Lett.* **104**, 106408 (2010).
- [18] S. Nakatsuji, Y. Machida, Y. Maeno, T. Tayama, T. Sakakibara, J. van Duijn, L. Balicas, J. N. Millican, R. T. Macaluso, and Julia Y. Chan, *Phys. Rev. Lett.* **96**, 087204 (2006).
- [19] B. J. Kim, H. Ohsumi, T. Komesu, S. Sakai, T. Morita, H. Takagi, and T. Arima, *Science* **323**, 1329 (2009).
- [20] Y. Okamoto, M. Nohara, H. Aruga-Katori, and H. Takagi, *Phys. Rev. Lett.* **99**, 137207 (2007); M. J. Lawler, H. Y. Kee, Y. B. Kim, and A. Vishwanath, *Phys. Rev. Lett.* **100**, 227201 (2008).
- [21] D. A. Pesin and L. Balents, *Nature Phys.* **6**, 376 (2010).
- [22] H.-M. Guo and M. Franz, *Phys. Rev. Lett.* **103**, 206805 (2009); B. J. Yang and Y. B. Kim, *Phys. Rev. B* **82**, 085111 (2010); M. Kargarian, J. Wen, and G. A. Fiete, *Phys. Rev. B* **83**, 165112 (2011).
- [23] X. Wan, A. M. Turner, A. Vishwanath, and S. Y. Savrasov, *Phys. Rev. B* **83**, 205101 (2011).
- [24] H. Kuriyama, J. Matsuno, S. Niitaka, M. Uchida, D. Hashizume, A. Nakao, K. Sugimoto, H. Ohsumi, M. Takata, and H. Takagi, *Appl. Phys. Lett.* **96**, 182103 (2010).
- [25] A. M. Turner, Y. Zhang, R. S. K. Mong, and A. Vishwanath, [arXiv:1010.4335](https://arxiv.org/abs/1010.4335) [*Phys. Rev. B* (to be published)].
- [26] T. L. Hughes, E. Prodan, and B. A. Bernevig, *Phys. Rev. B* **83**, 245132 (2011).
- [27] S. Y. Savrasov, *Phys. Rev. B* **54**, 16470 (1996).
- [28] V. I. Anisimov, F. Aryasetiawan, and A. I. Lichtenstein, *J. Phys. Condens. Matter* **9**, 767 (1997).
- [29] G. Kotliar, S. Y. Savrasov, K. Haule, V. S. Oudovenko, O. Parcollet, and C. A. Marianetti, *Rev. Mod. Phys.* **78**, 865 (2006).
- [30] W. Witczak-Krempa and Y. B. Kim, *Phys. Rev. B* **85**, 045124 (2012).
- [31] K. Tomiyasu *et al.*, [arXiv:1110.6605](https://arxiv.org/abs/1110.6605).
- [32] See Supplemental Material at <http://link.aps.org/supplemental/10.1103/PhysRevLett.108.146601> for our structural and chemical stability checks of the proposed osmium spinel compounds.
- [33] R. Arita, J. Kuneš, A. V. Kozhevnikov, A. G. Eguluz, and M. Imada, *Phys. Rev. Lett.* **108**, 086403 (2012).
- [34] M. Elhajal, B. Canals, R. Sunyer, and C. Lacroix, *Phys. Rev. B* **71**, 094420 (2005).
- [35] G. Jackeli and G. Khaliullin, *Phys. Rev. Lett.* **102**, 017205 (2009); Jiri Chaloupka, G. Jackeli, and G. Khaliullin, *Phys. Rev. Lett.* **105**, 027204 (2010).
- [36] D. Mandrus, J. R. Thompson, R. Gaal, L. Forro, J. C. Bryan, B. C. Chakoumakos, L. M. Woods, B. C. Sales, R. S. Fishman, and V. Keppens, *Phys. Rev. B* **63**, 195104 (2001); D. J. Singh, P. Blaha, and K. Schwarz, and J. O. Sofo, *Phys. Rev. B* **65**, 155109 (2002).
- [37] L. C. Chapon, P. Manuel, F. Damay, P. Toledano, V. Hardy, and C. Martin, *Phys. Rev. B* **83**, 024409 (2011); S. E. Dutton, E. Climent-Pascual, P. W. Stephens, J. P. Hodges, A. Huq, C. L. Broholm, and R. J. Cava, *J. Phys. Condens. Matter* **23**, 246005 (2011).
- [38] A. H. Castro Neto, F. Guinea, N. M. R. Peres, K. S. Novoselov, and A. K. Geim, *Rev. Mod. Phys.* **81**, 109 (2009).
- [39] R. Li, J. Wang, X. L. Qi, and S. C. Zhang, *Nature Phys.* **6**, 284 (2010); J. Wang, R. Li, S. C. Zhang, and X. L. Qi, *Phys. Rev. Lett.* **106**, 126403 (2011).